DLR-IRIDeS Joint Workshop on Remote Sensing and Multi-Risk Modeling for Disaster Management, 19 September 2014, Bonn, Germany

Detection of exterior damage of buildings from high-resolution SAR images

September 19, 2014

Fumio Yamazaki[a)], Yoji Iwasaki[b)], Wen Liu[c)], Takashi Nonaka[d)] and Tadashi Sasagawa[d)]

a) Professor, Graduate School of Engineering, Chiba University, Japan.

b) Civil Engineer, Chiba Prefectural Government, Japan.

c) JSPS Research Fellow, Tokyo Institute of Technology, Japan.

d) Satellite Business Division, PASCO Corporation, Tokyo, Japan.

Wavelength of Electromagnetic Waves and Satellite Sensors

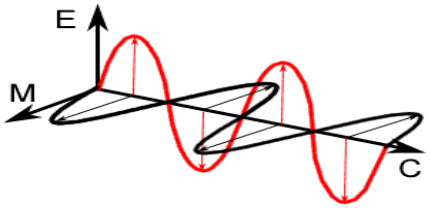

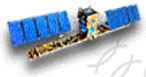

Reflection ***Radiation*** ***Active***

γ-ray, x-ray | UV | Visible | Infrared | Microwave

Visible Infrared

(μm) 0.40 0.50 0.60 0.70 0.80 10.4 13.5

Wavelength

LANDSAT/MSS
空間分解能:80m

0.50 0.60 0.70 0.80 1.1
1 2 3 4

LANDSAT/TM
空間分解能:30m, B6:120m

0.45 0.52 0.60 0.63 0.69 0.75 0.90 1.55 1.75 2.08 2.35 10.4 12.5
1 2 3 4 5 7 6

B **G** **R** **NIR** Mid-IR Thermal

TERRA/ASTER
空間分解能:B1-B3:15m, B4-B9:30m
B10-B14:90m

0.52 0.60 0.63 0.69 0.76 0.86 1.6 1.7 2.145 2.43 8.125 11.65
1 2 3 4 5 6 7 8 9 10 12 13 14

Platforms of Remote Sensing

- **Satellite**: near-polar orbit, geo-stationary, Space Shuttle
- **Airborne platform**: airplane, helicopter, UAV
- **Ground-based**: balloon, tall building, crane, ladder

Platforms of Remote Sensing

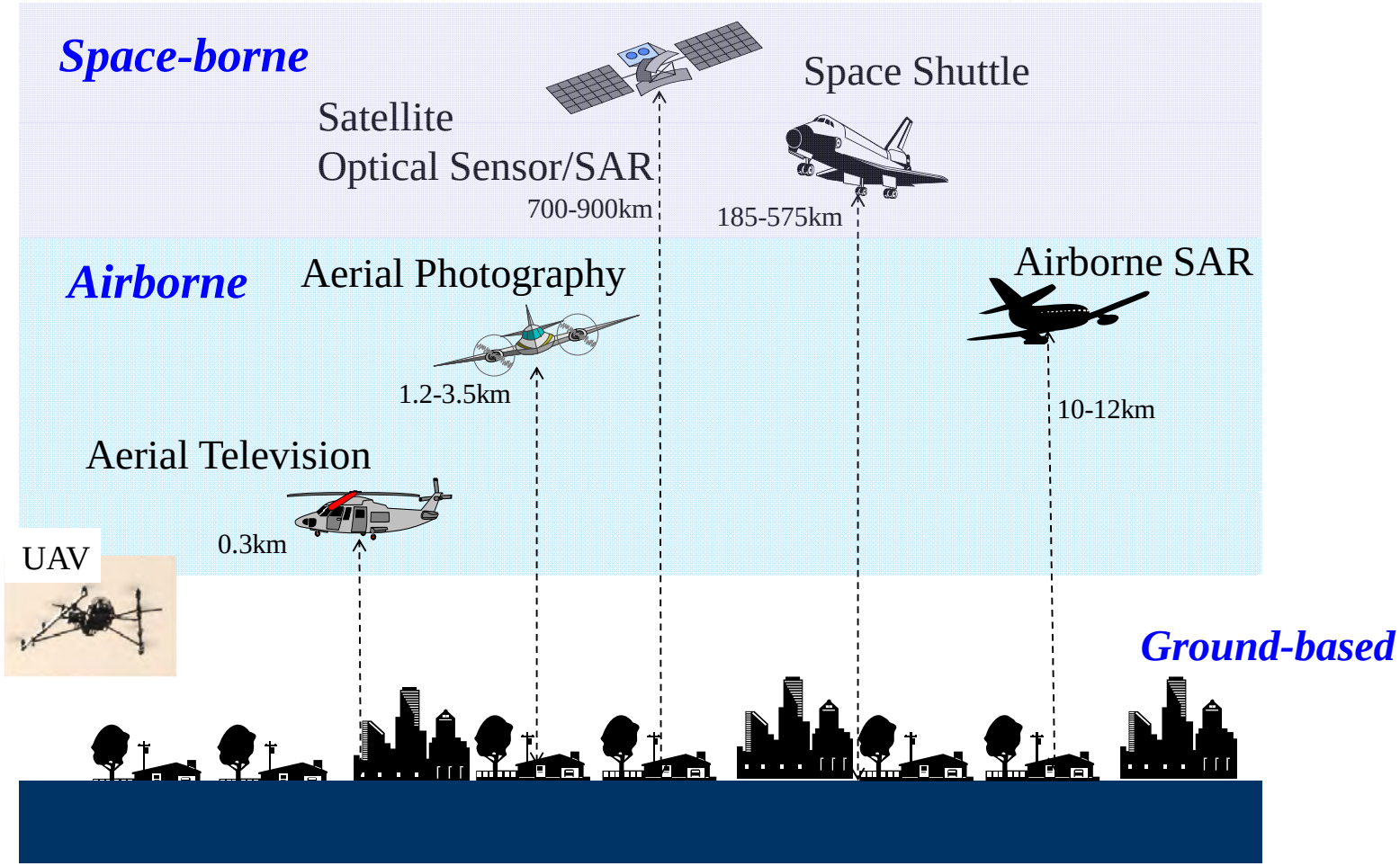

Acquisition condition of various sensors and platforms in disaster response

Platform /Sensor	Satellite ◎ Large coverage	Airborne ○ Mod. coverage	Ground Based △ Low coverage
Optical Sensor	△ Day, Fixed time △ No cloud	○Day, Any time ○ No low cloud	◎ Day, Any time
Lidar	×	○ Day, Any time ○ No low cloud	◎ Day, Any time
Thermal Infrared	○All day, Fixed time △ No cloud △ Low resolution	◎ All day, Any time ○ No low cloud ○ Mod. resolution	◎All day, Any time ◎ High resolution
SAR	○ All day, Fixed time ◎ All weather	◎ All day, Any time ◎ All weather △ R & D stage	×

Satellites that observed the 2011 Tohoku earthquake

Optical, Medium Resolution

- ALOS AVNIR-2 (10m)
- Terra ASTER (15m)
- Landsat 7 (30m)

Optical, High Resolution

- FORMOSAT-2 (2.0m)
- THEOS (2.0m)
- RapidEye (2.5m)
- WorldView-1,2 (0.5m)
- QuickBird (0.6m)
- Ikonos (1.0m)
- GeoEye-1 (0.5m)

SAR

- ALOS PALSAR (L-band, 6.25m)
- Radarsat 1, 2 (C-band, 8m)
- TerraSAR-X (X-band, 3m)
- COSMO-SkyMed (X-band, 3m)

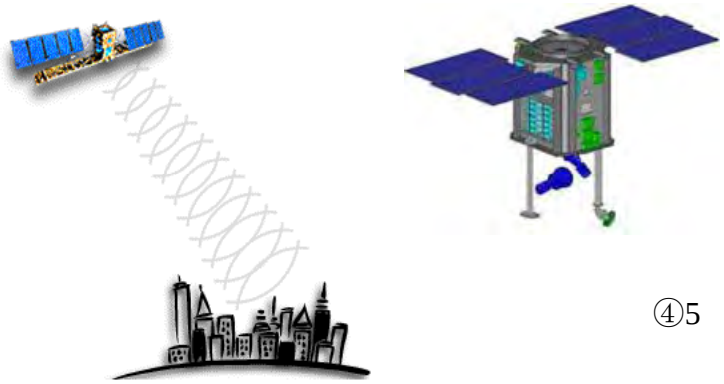

Flow of post-event damage assessment

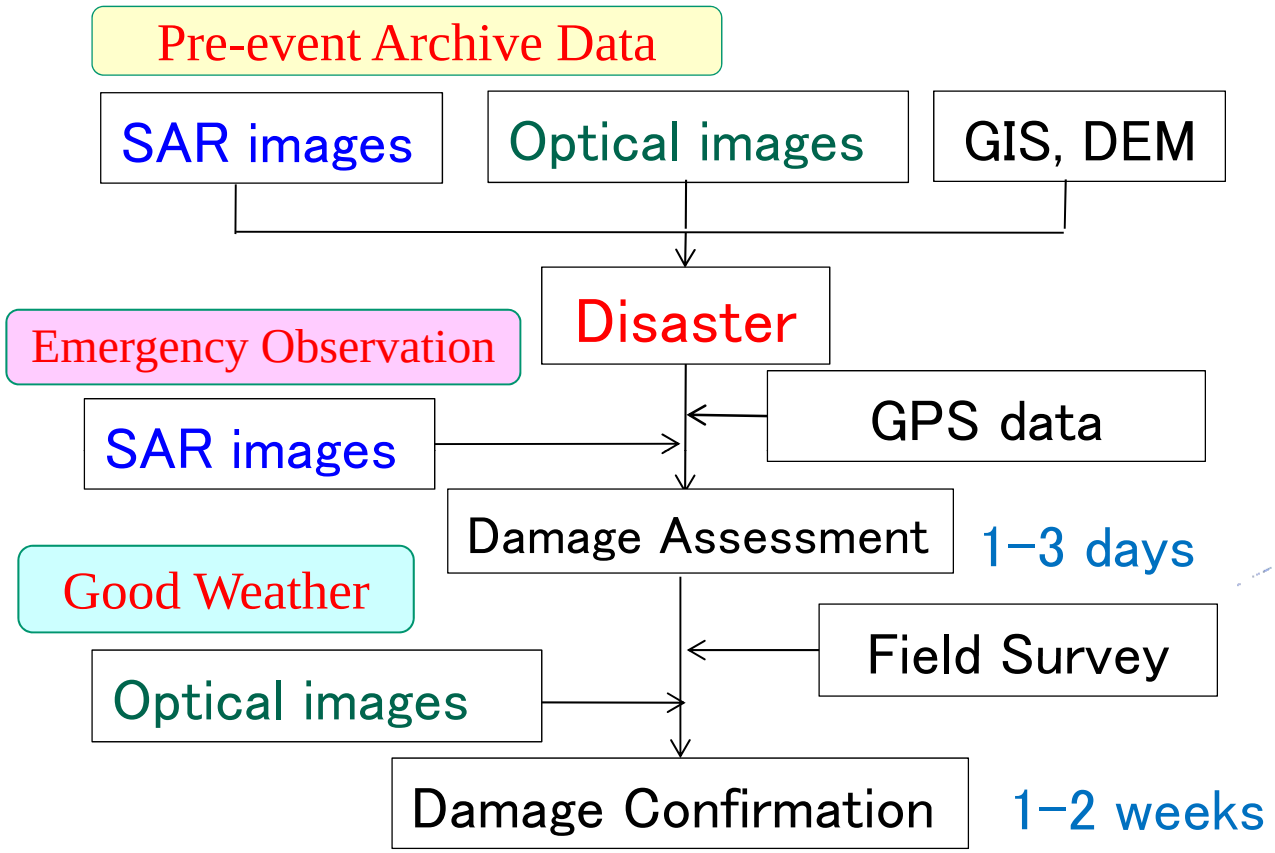

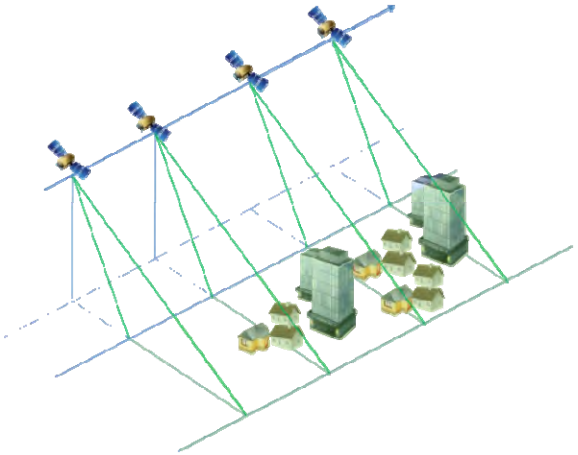

Characteristics of SAR

- All Weather, Daytime and Nighttime
- Combined use with GIS and Optical images
- Include height and lateral information due to side-looking mode

Typical tsunami damage to reinforced concrete and steel-frame buildings observed in our field survey after the 2011 Tohoku, Japan, earthquake

Onagawa

Minami-Sanriku

Ohtsuchi

The damage was concentrated to exterior walls and lower stories of buildings.

Background

Building damage such as to exterior walls or mid-story collapse is often overlooked in vertical optical satellite images.

Objectives of the Research

Utilizing the side-looking nature of SAR, the change in the backscattering coefficient σ_0 within the layover area of an individual building is investigated to detect the damage situation of its exterior wall due to the 2011 Tohoku, Japan, earthquake and tsunami.

Scheme of SAR observation for a tall flat-roof building

TSX intensity image of central Tokyo

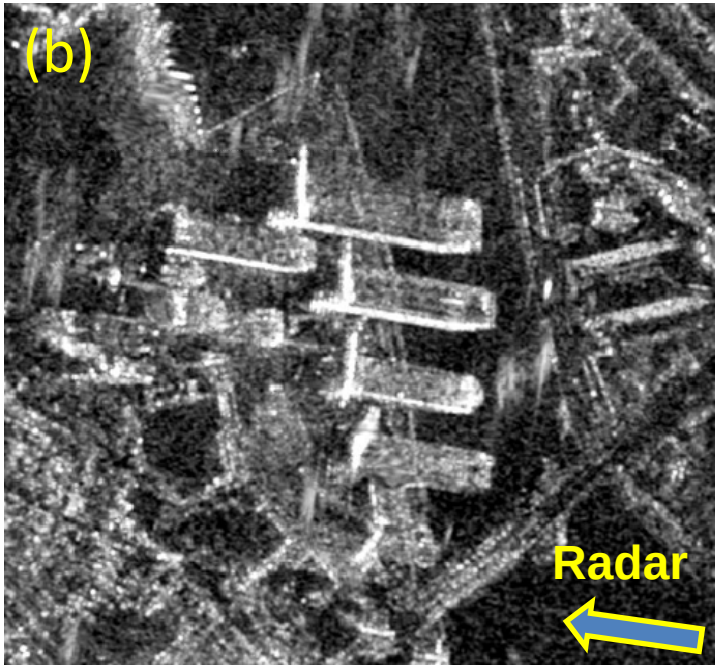

3D layout

(a)

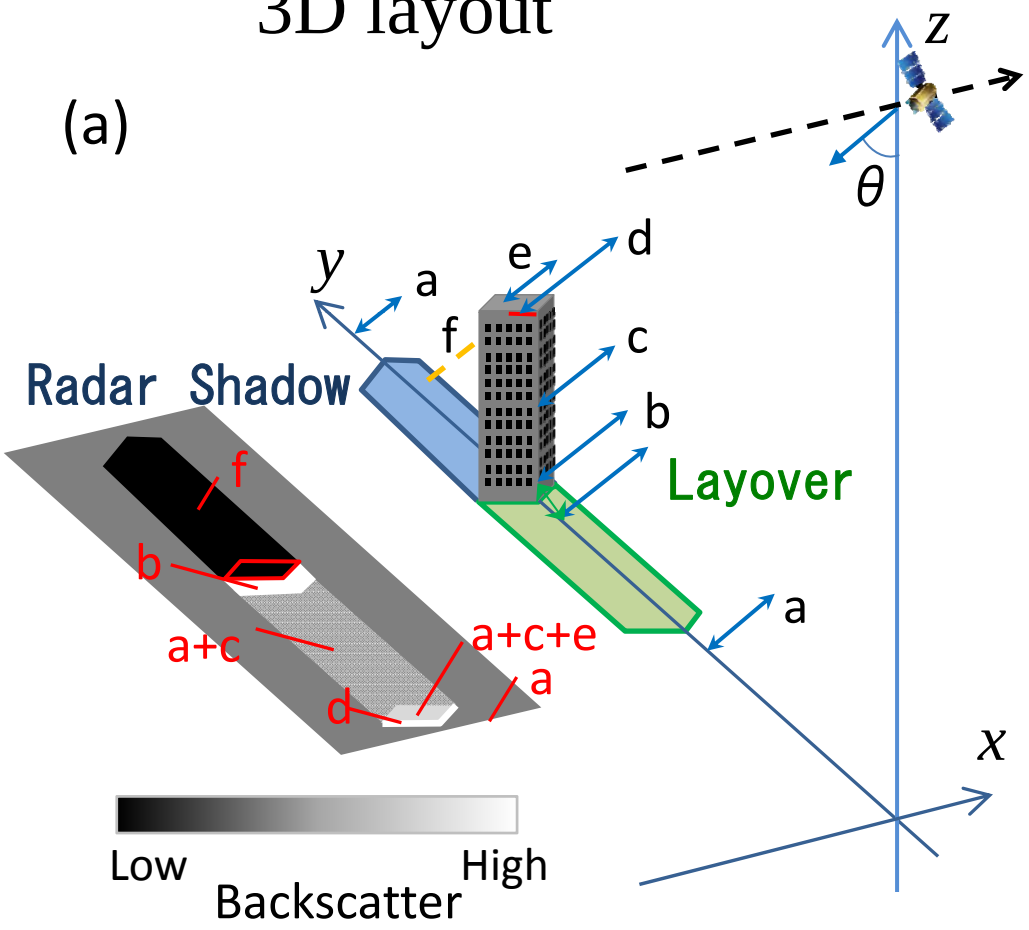

$$L = H/\tan\theta \quad L' = H\tan\theta$$

Amplitude of backscatter from an intact building (c), and a damaged building due to tsunami (d).

Before Tsunami

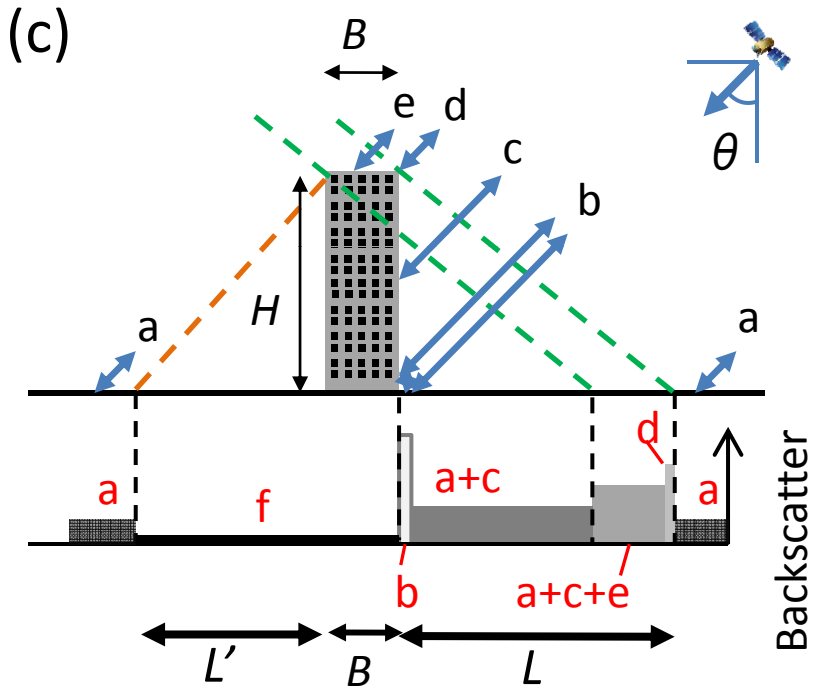

After Tsunami

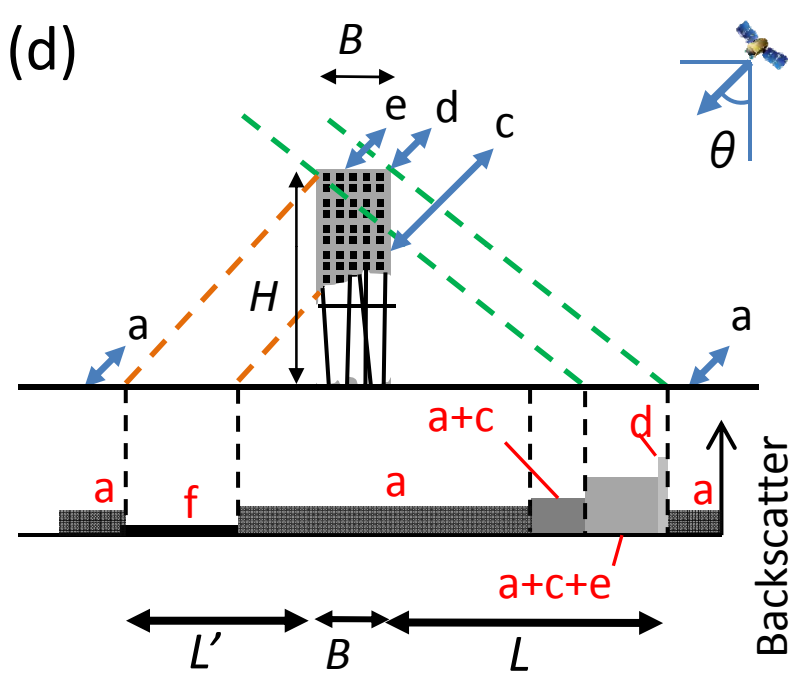

Radar Shadow

$$L' = H \tan\theta$$

Layover

$$L = H/\tan\theta$$

TerraSAR-X images along the Pacific coast of Tohoku including the Sendai-Shiogama Port

(a) 2010/10/21 05:43

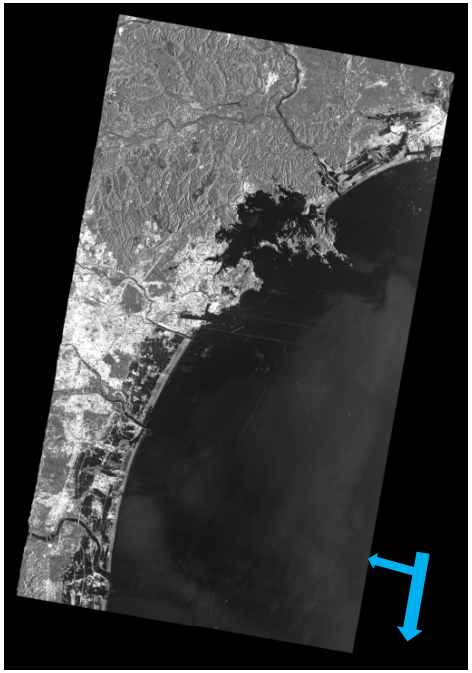

(b) 2011/03/13 05:43

(c) 2011/04/04 05:43

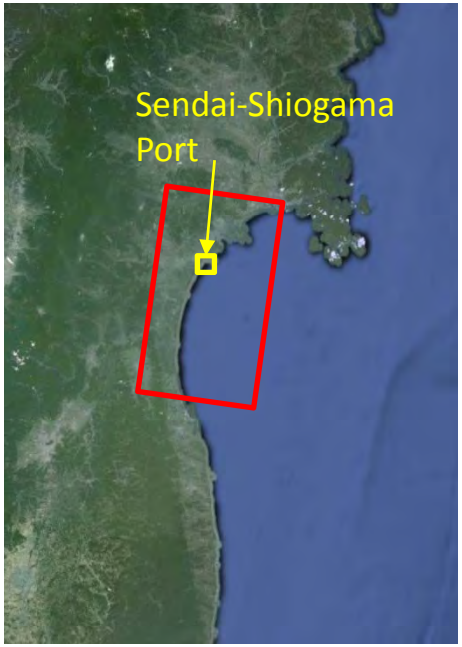

(d) TSX's Imaging Area

	a	b	c	
Date	2010.10.21	2011.03.13	2011.04.04	
Incident Angle	37.316°	37.301°	37.317°	
Heading Angle	190.027°	190.029°	190.025°	
Mode	StripMap (R 3.01 m x A 3.04 m)			
Polarization	HH			
Product	EEC_SE (1.25 m/pixel)			

Transformed to Sigma Naught (σ^0)

Enhanced Lee filter (3 x 3 pixels)

Detection of flooded areas & Extraction of crustal movement

G&B: 2010.10.21 R: 2011.03.13

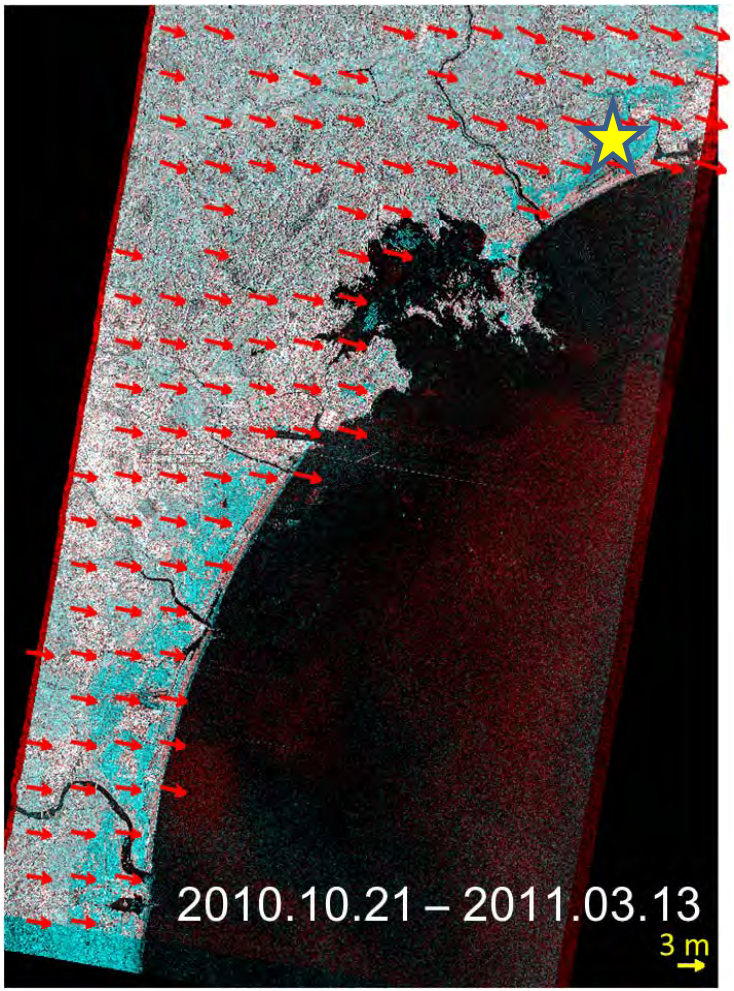

Pre-event

Post-event

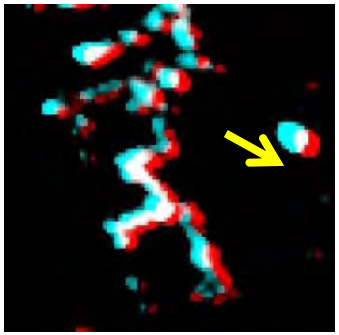

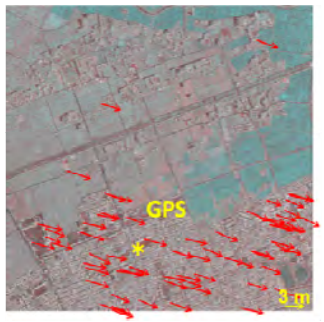

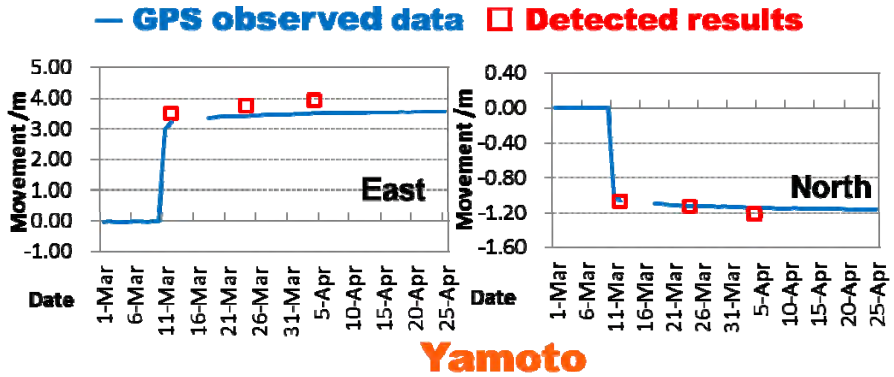

W. Liu, F. Yamazaki, Detection of Crustal Movement from TerraSAR-X intensity images for the 2011 Tohoku, Japan Earthquake, ***Geoscience and Remote Sensing Letters***, IEEE, 10(1), 2013.

W. Liu, F. Yamazaki, H. Gokon, S. Koshimura, Extraction of Tsunami-Flooded Areas and Damaged Buildings in the 2011 Tohoku-Oki Earthquake from TerraSAR-X Intensity Images, ***Earthquake Spectra***, 29(S1), 2013.

Aerial images of Sendai-Shiogama Port and its surroundings after the tsunami attack.

Area **A** within the tsunami inundation zone

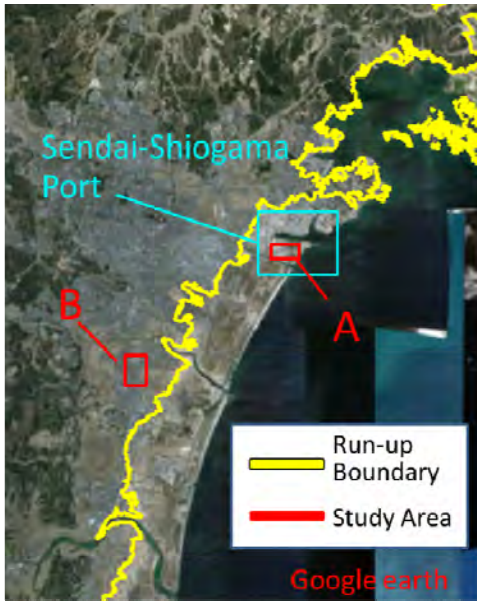

Aerial images of Sendai-Shiogama Port and its surroundings after the tsunami attack.

Area **B** : outside of the tsunami zone.

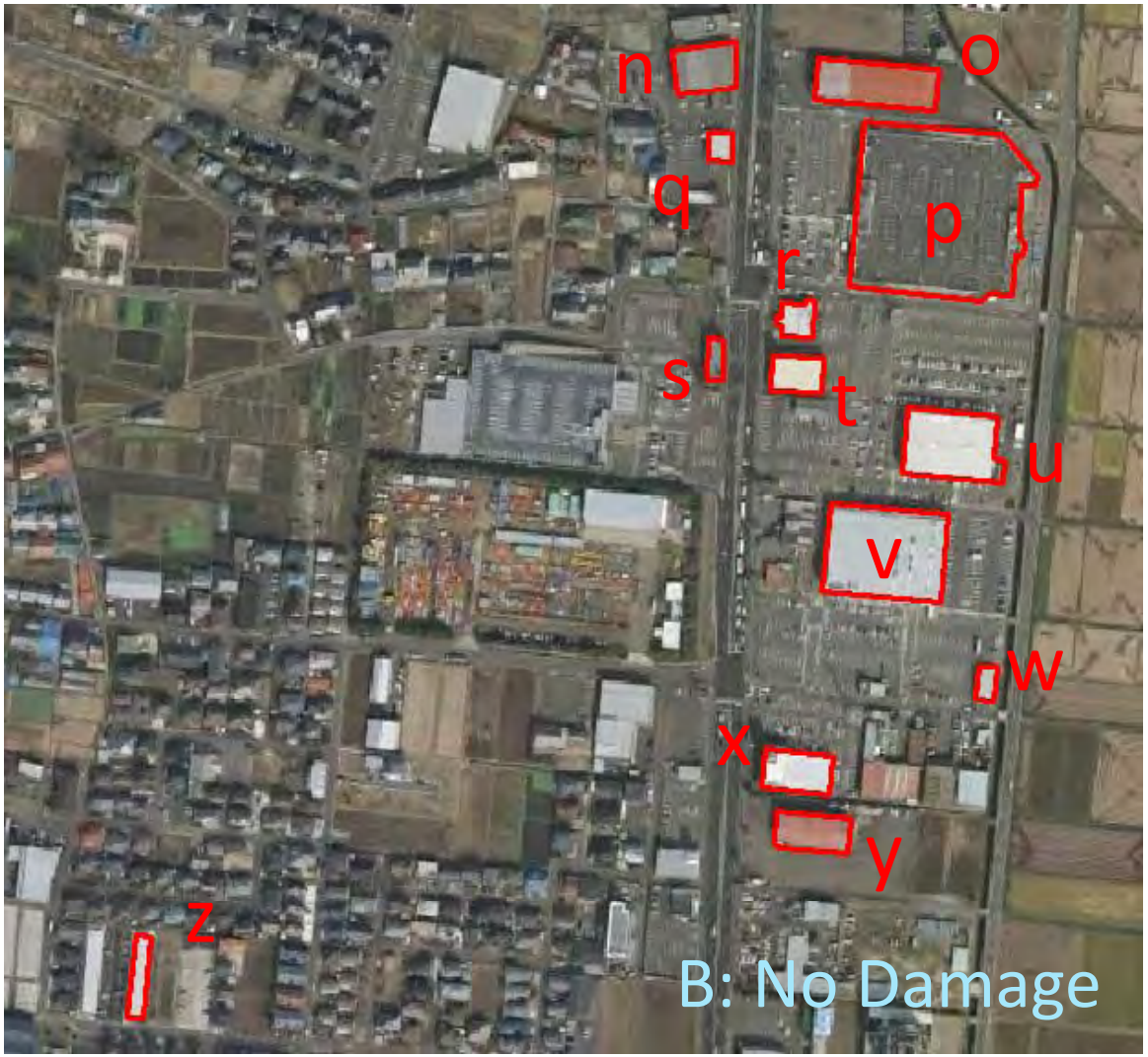

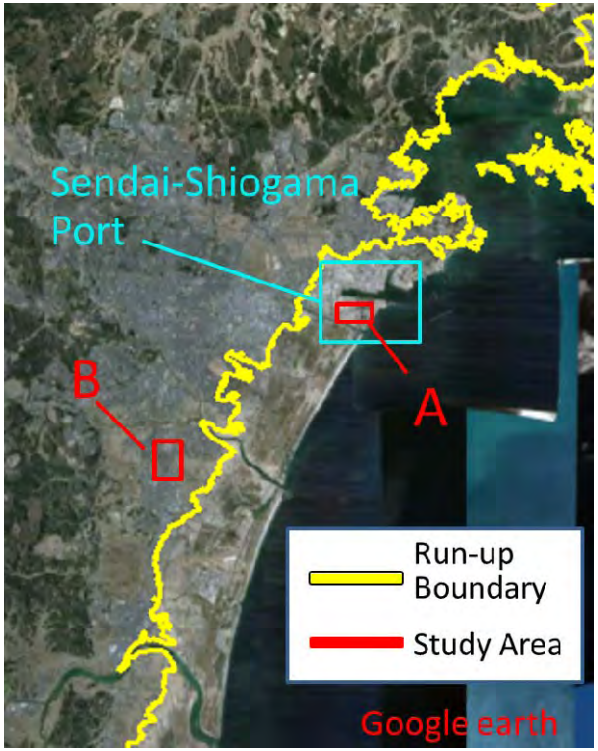

Average value of σ_0 within the layover area of each building for 13 damaged buildings at 3 time instants of SAR image acquisition.

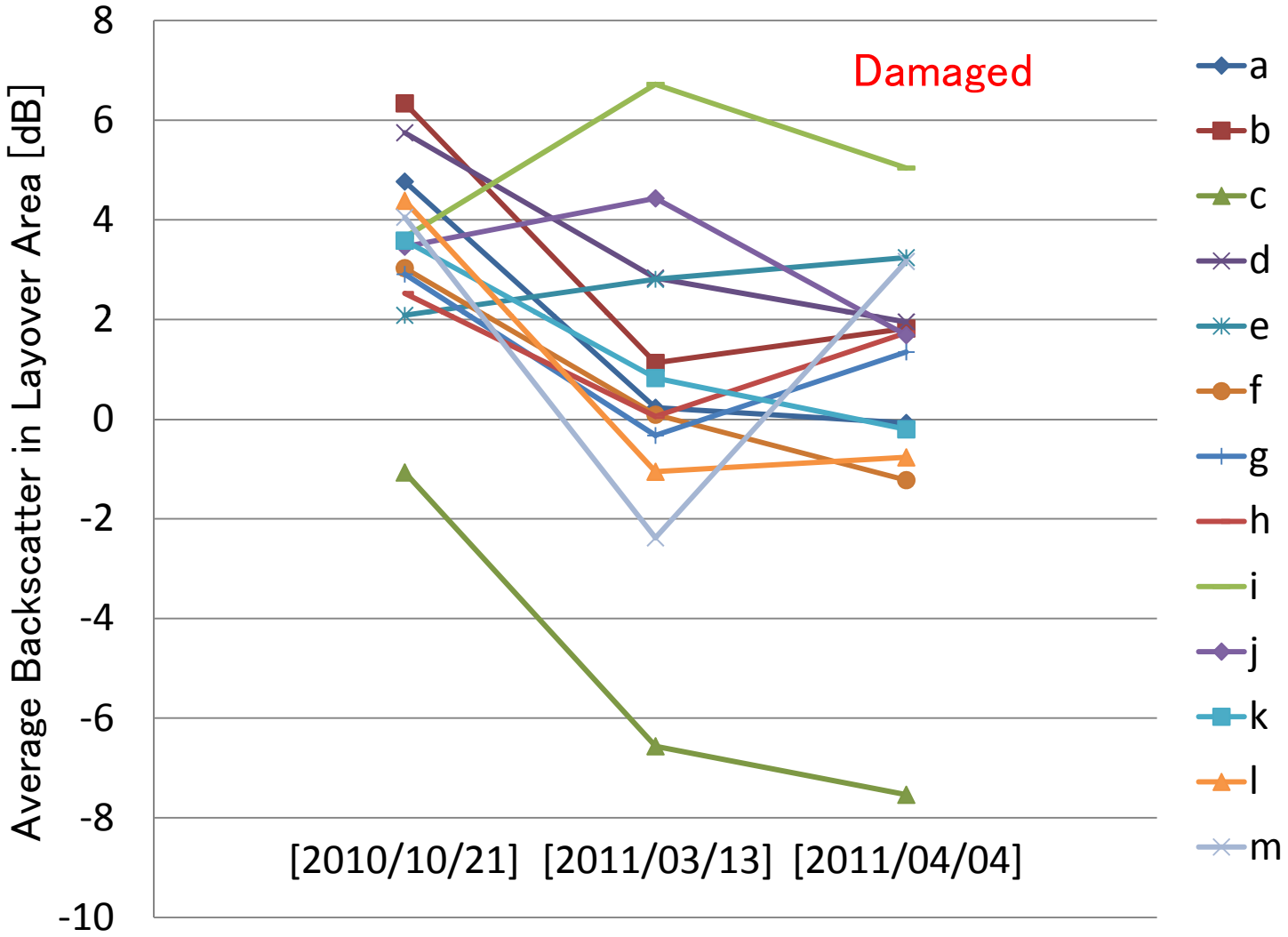

Average value of σ_0 within the layover area of each building for 13 non-damaged buildings at 3 time instants of SAR image acquisition

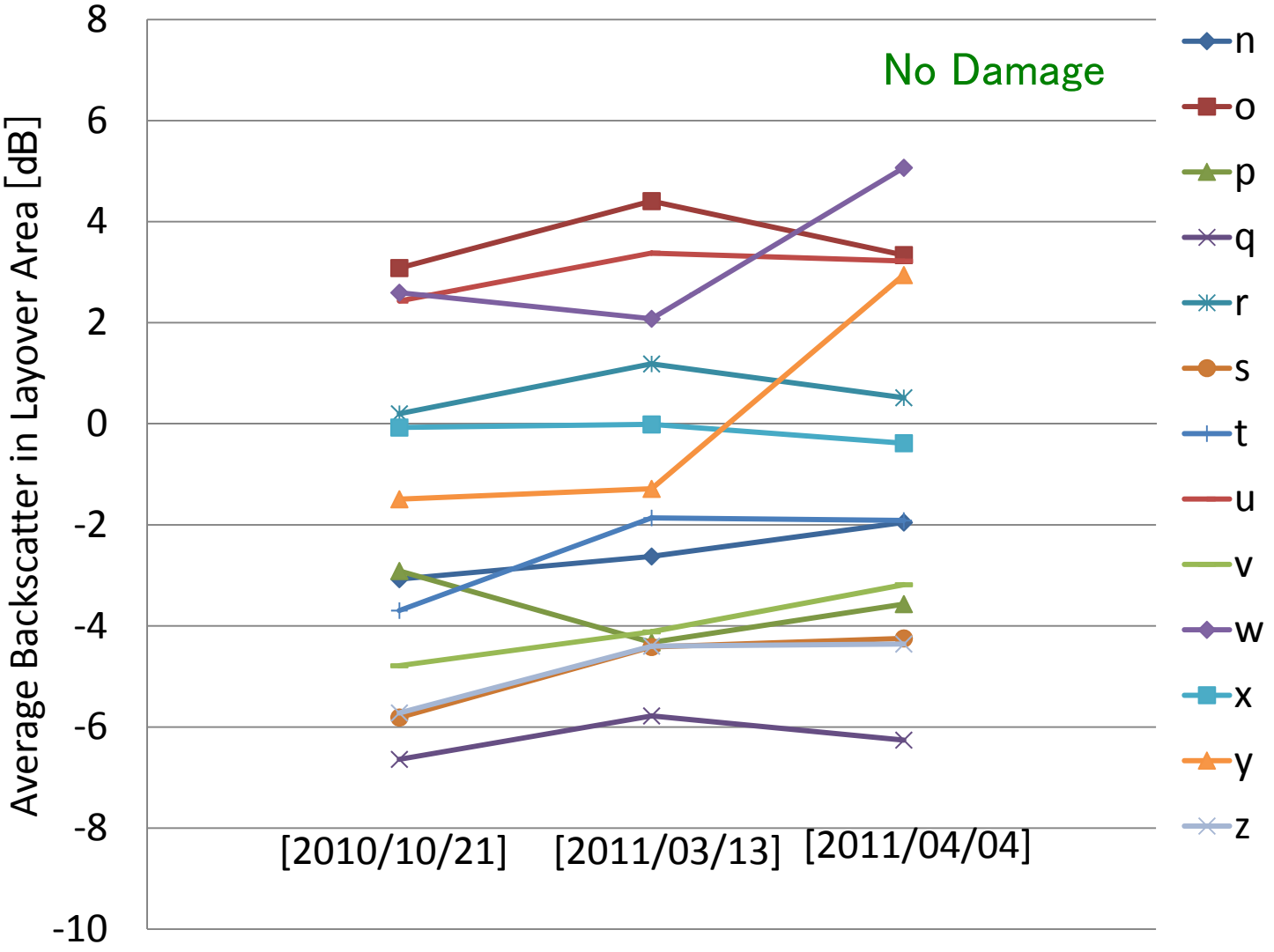

The difference of the average values of σ_0 within the layover area of each building before and after the tsunami attack

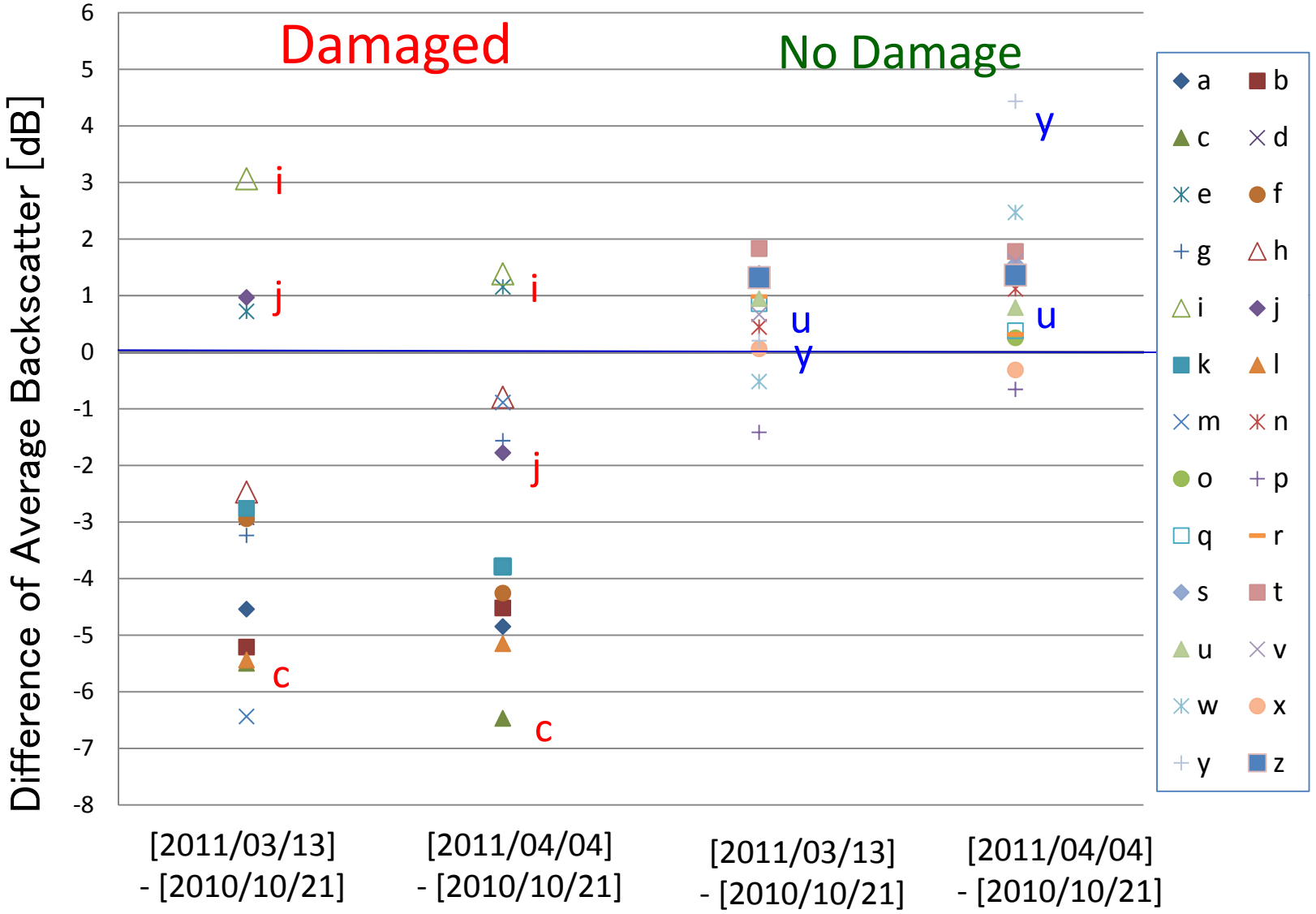

Close-up of the TSX images at the three acquisition dates and the optical images of similar acquisition times for damaged building c

c

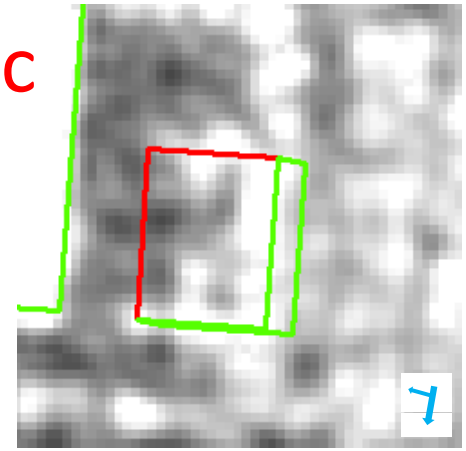

2010/10/21

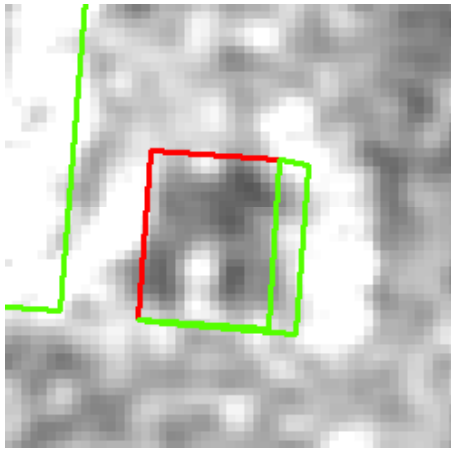

2011/03/13

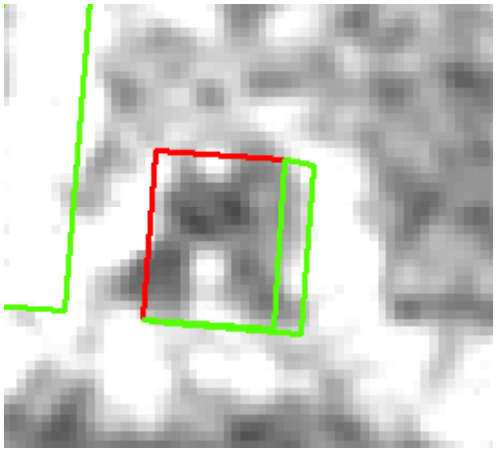

2011/04/04

— Building Footprint
— Layover Area

2010/04/04 GeoEye

2011/03/13 GeoEye

2011/04/06 ZENRIN

SAR Incident Side

Reduced σ_0

		平均値	標準偏差	平均値の差（事後—事前）	標準偏差の差（事後—事前）
c	2010/10/21	-1.07	3.76		
	2011/03/13	-6.56	4.45	-5.49	0.69
	2011/04/04	-7.54	3.71	-6.47	-0.04

Close-up of the TSX images at the three acquisition dates and the optical images of similar acquisition times for damaged building i

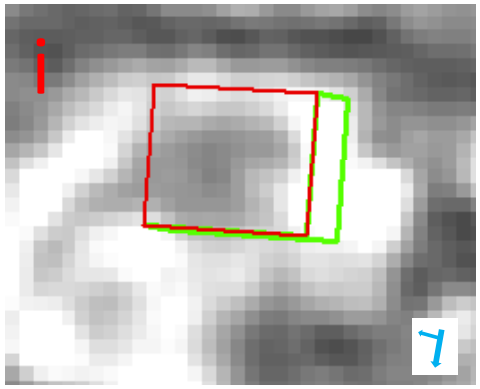

2010/10/21

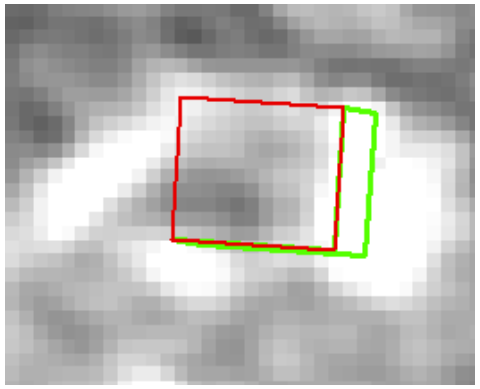

2011/03/13

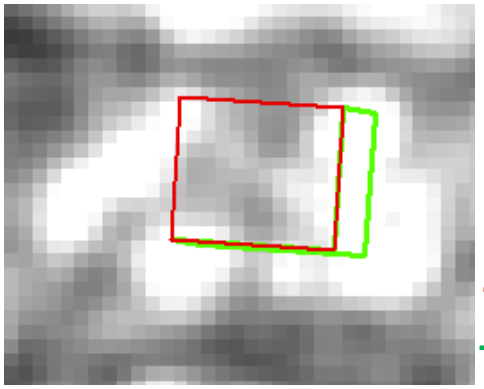

2011/04/04

— Building Footprint
— Layover Area

2010/04/04 GeoEye

2011/03/13 GeoEye

2011/04/06 ZENRIN

SAR Incident Side

Increased σ_0 on 3/13 and 4/4

Relatively small damage to exterior wall but steel frames are exposed.
Spread of debris on 3/13 but cleared on 4/04.

Close-up of the TSX images at the three acquisition dates and the optical images of similar acquisition times for damaged building j

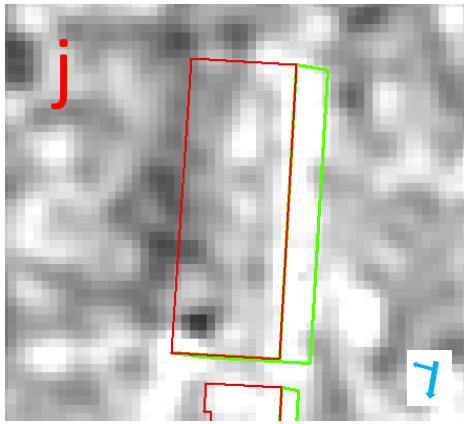

2010/10/21

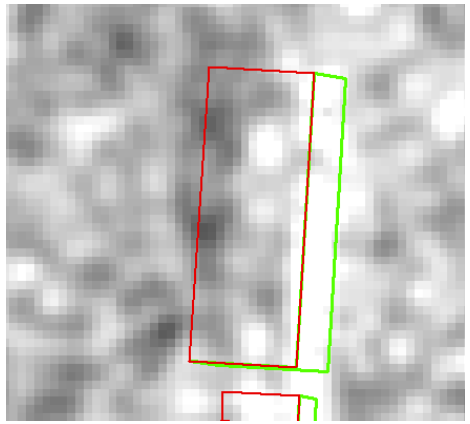

2011/03/13

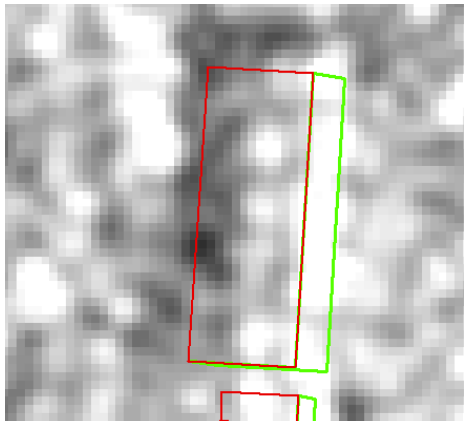

2011/04/04

— Building Footprint
— Layover Area

2010/04/04 GeoEye

2011/03/13 GeoEye

2011/04/06 ZENRIN

SAR Incident Side

Increased σ_0 on 3/13

Relatively small damage to exterior wall.

Spread of debris on 3/13 but cleared on 4/04.

Close-up of the TSX images at the three acquisition dates and the optical images of similar acquisition times for no damage building u

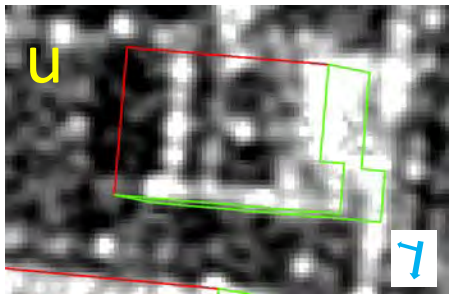

2010/10/21

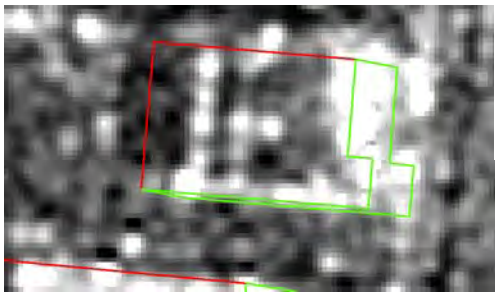

2011/03/13

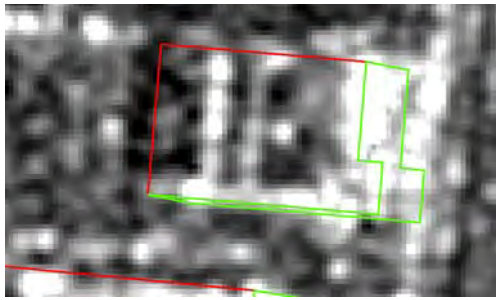

2011/04/04

— Building Footprint
— Layover Area

2010/04/04 GeoEye

2011/03/13 GeoEye

2011/04/06 ZENRIN

SAR Incident Side

No damage.

σ_0 was almost no change.

		平均値	標準偏差	平均値の差（事後—事前）	標準偏差の差（事後—事前）
u	2010/10/21	2.43	8.25		
	2011/03/13	3.38	8.23	0.95	-0.02
	2011/04/04	3.22	8.17	0.79	-0.09

Close-up of the TSX images at the three acquisition dates and the optical images of similar acquisition times for no damage building y

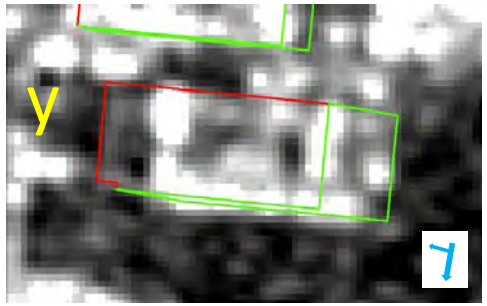

2010/10/21

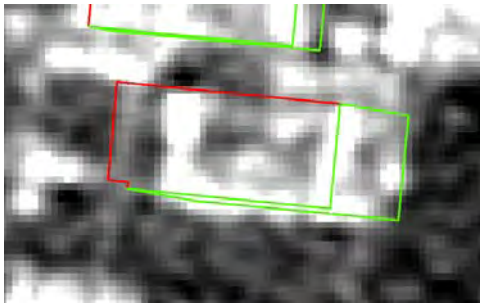

2011/03/13

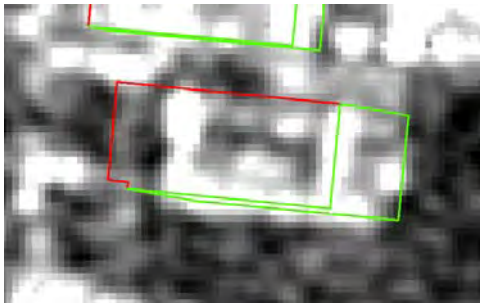

2011/04/04

Building Footprint
Layover Area

2010/04/04 GeoEye

2011/03/13 GeoEye

2011/04/06 ZENRIN

SAR Incident Side

No damage.

σ_0 increased on 4/04. Maybe due to parking cars?

Fukushima Daiichi nuclear power plant in September 2011

#1 reactor building

#2 reactor building

#3 reactor building

#4 reactor building

Photos by TEPCO on 2011/09/15

GeoEye-1 2011/09/16

TerraSAR-X images of Fukushima Daiichi NPP

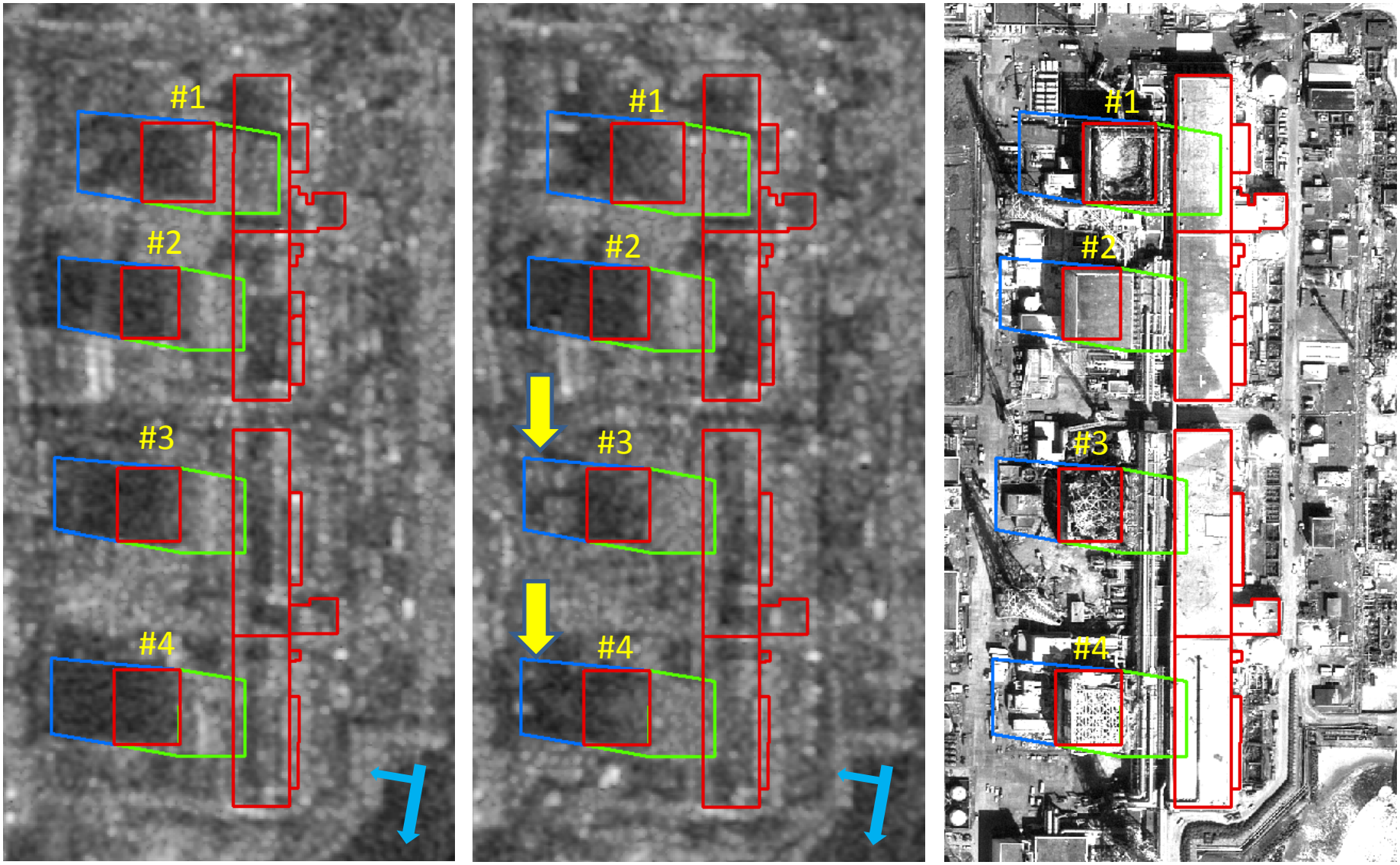

TSX 2011/03/13 05:43 TSX 2011/09/05 05:43 GeoEye-1 2011/09/16 09:33

Layover Radar Shadow Building Footprint

Conclusions

- Multi-temporal TerraSAR-X images covering the Sendai-Shiogama Port in the 2011 Tohoku, Japan earthquake were employed to detect building damage due to tsunamis.
- The average value of backscattering coefficients in the layover area of each building was seen to reduce for damaged buildings in the post-event images due to the reduced backscatter from its exterior walls
- On the contrary, no much change was seen for most of the non-damaged buildings.
- This example indicates the usefulness of high-resolution SAR images to detect severe damage to building exterior walls from the changes of the backscattering coefficient in layover areas.

Thank you very much!

Miracle single pine tree
in Rikuzen-Takada